Systematics of the dipole polarizability

TECHNISCHE UNIVERSITÄT DARMSTADT

Outline:

- Inelastic proton scattering
- Research Center for Nuclear Physics
- The case of ^{58}Ni:
  - State-by-state analysis
  - Multipole decomposition analysis
- Dipole polarizability
- Summary and outlook

SFB 1245

Supported by the Deutsche Forschungsgemeinschaft (DFG, German Research Foundation)
Project-ID 279384907 - SFB 1245.

Introduction

- Inelastic proton scattering at
  - Scattering angles close to 0°
  - Proton energies of ≈ 300 MeV
- Kinematics favours excitation of
  - Electric dipole transitions
  - Isovector-spinflip M1 transitions
- Consistent measurement below and above the particle separation threshold

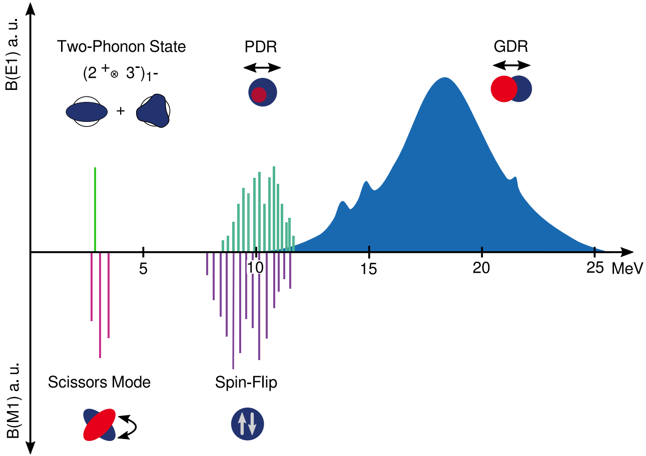

Introduction

- Inelastic proton scattering at
  - Scattering angles close to 0°
  - Proton energies of ≈ 300 MeV
- Kinematics favours excitation of
  - Electric dipole transitions
  - Isovector-spinflip M1 transitions
- Consistent measurement below and above the particle separation threshold

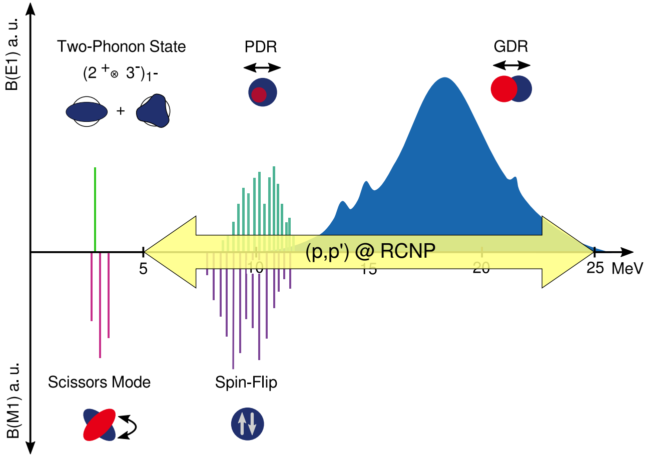

Electric dipole transitions in (p,p')

- Relativistic Coulomb excitation
- Virtual photon method

$$\frac{d^2\sigma_{E1}}{d\Omega dE} = \frac{1}{E}\frac{dN_{E1}}{d\Omega}\sigma_{abs}^{E1}$$

$$\frac{dB(E1)}{dE} = \frac{9\hbar c}{16\pi^2}\frac{\sigma_{abs}^{E1}}{E}$$

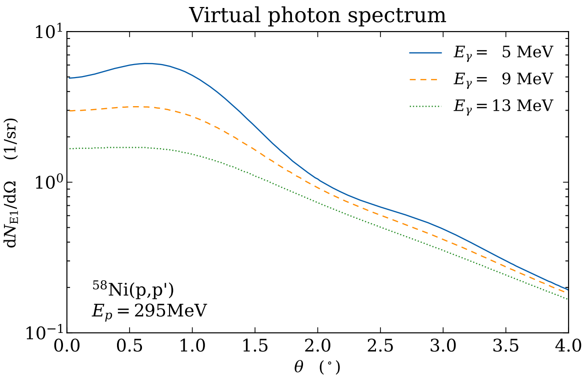

Dipole polarizability

- Dipole polarizability

$$\alpha_D = \frac{\hbar c}{2\pi^2} \int \frac{\sigma^{E1}_{abs}}{E^2} dE$$

- Correlated to
  - Neutron skin thickness
  - Symmetry energy
- Systematics over isotopic chains: $^{40,48}Ca$, ^{68}Ni, ^{90}Zr, stable even mass Sn, ^{208}Pb

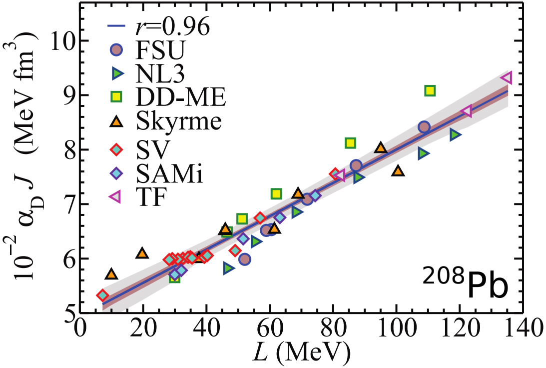

X. Roca-Maza et al., Phys. Rev. C88, 024316 (2013)

Magnetic dipole transitions in (p,p')

- Isovector spin-flip M1 transitions
- Isospin analog to Gamow-Teller transition

$$B(\mathrm{GT}) = \frac{C_{\mathrm{GT}}^2}{2(2T_f+1)} |\langle f||| \sum_k^A \sigma_k \tau_k |||i\rangle|^2$$

$$B(\mathrm{M1}_{\sigma\tau}) = \frac{C_{\mathrm{M1}}^2}{4(2T_f+1)} |\langle f||| \sum_k^A \sigma_k \tau_k |||i\rangle|^2$$

- Unit cross section method with $\hat{\sigma}_{\mathrm{M1}} \approx \hat{\sigma}_{\mathrm{GT}}$

$$\frac{\mathrm{d}\sigma_{\mathrm{M1}}^{\mathrm{IV}}}{\mathrm{d}\Omega}(0^\circ) = \hat{\sigma}_{\mathrm{M1}} F_{\mathrm{M1}}(0^\circ, E_x) B(\mathrm{M1}_{\sigma\tau})$$

J. Birkhan et al., Phys. Rev. C 93, 041302(R) (2016)

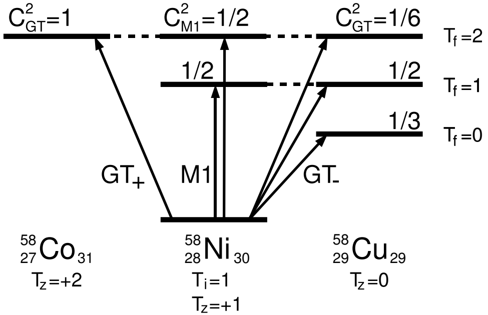

H. Fujita et al., Phys. Rev. C 75, 034310 (2007)
Y. Fujita et al., Prog. Part. Nucl. Phys. 66, 549 (2011)

Research Center for Nuclear Physics (RCNP)

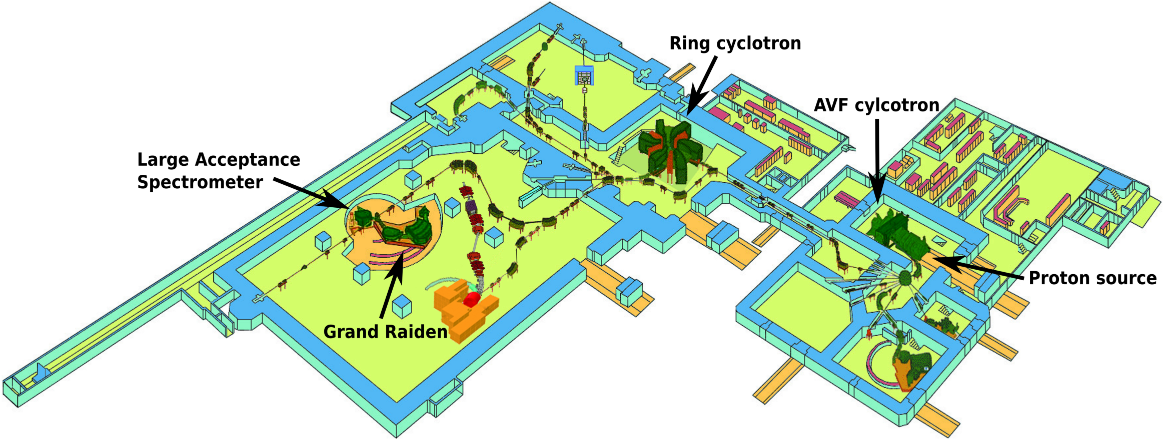

Experiment at Grand Raiden Spectrometer
^{58}Ni

- Proton beam with $E_p = 295\,\text{MeV}$
- Spectrometer angles:
  0°, 2.5°, and 4.5°
- Raw data analysis:
  H. Matsubara, Dissertation, Osaka University (2010)
- Excitation energy spectra for seven scattering angles between 0.4° and 5.15°

Spectrometer setup at 0°

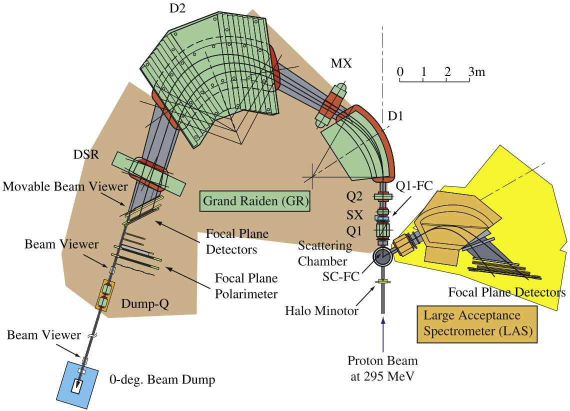

A. Tamii et al., Nucl. Instr. Meth A 605, 236 (2009)

^{58}Ni Spectra

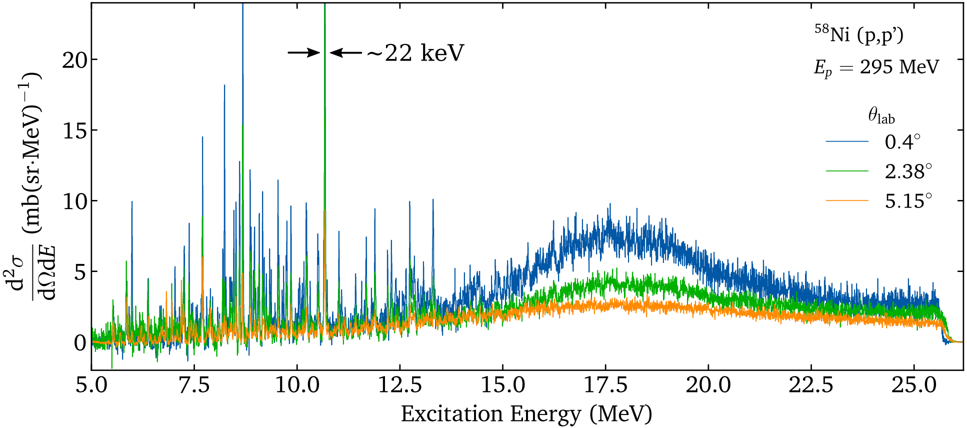

State-by-state analysis

- Statewise analysis between 5 MeV and 13.3 MeV
- 185 transitions found
  - 147 present in at least five spectra
- Multipolarities: Angular distributions
- DWBA calculations
  V. Yu. Ponomarev (2019)

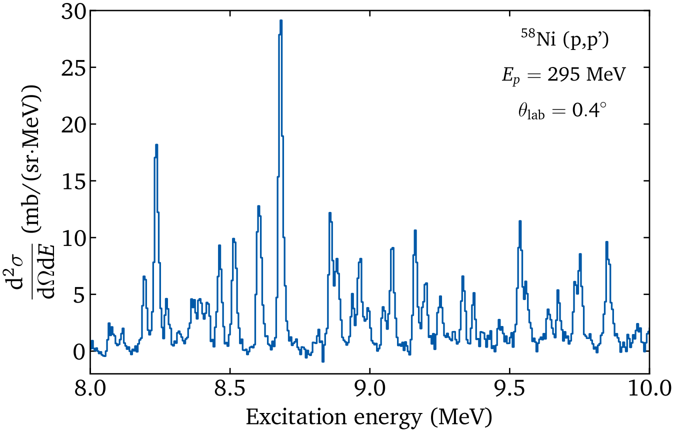

State-by-state analysis

- Identification of low energy M1 transitions works well

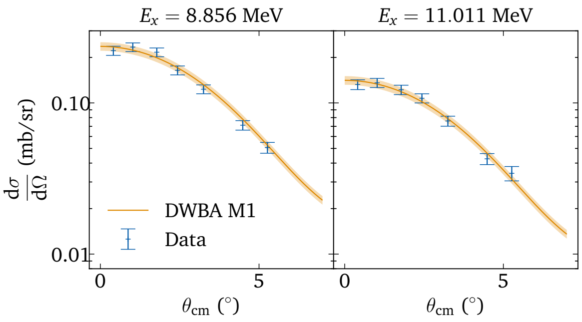

- Identification of low energy E1 transitions more difficult

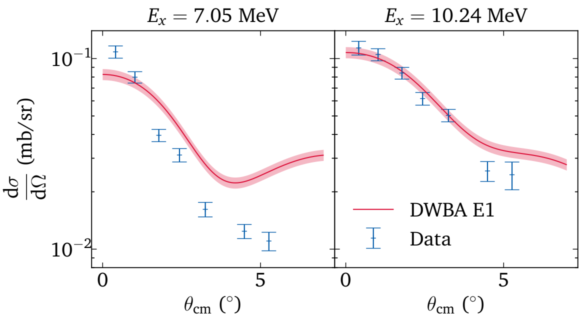

State-by-state analysis

- Dipole character from angular distributions
- Multipolarity unique from combination with other experiments

- Nuclear resonance fluorescence (γ,γ'):
  F. Bauwens et al., Phys. Rev. C 62, 024302 (2000)
  M. Scheck et al., Phys. Rev. C 88, 044304 (2013)
  J. Sinclair, priv. comm. (2019)

  E1, M1

- Inelastic electron scattering (e,e') :
  W.Mettner et al., Nucl. Phys. A473, 160 (1987)

  M1, M2

- (p,p') at 160 MeV + ^{58}Ni(^{3}He,t)^{58}Cu:
  H.Fujita et al., Phys. Rev. C 75, 034310 (2007)

  E1, IVSM1

State-by-state analysis

- Dipole character from angular distributions
- Multipolarity unique from combination with other experiments

^{58}Ni:

41 M1 transitions

40 E1 transitions

59 dipole transition

- Nuclear resonance fluorescence (γ, γ'):
  F. Bauwens et al., Phys. Rev. C 62, 024302 (2000)
  M. Scheck et al., Phys. Rev. C 88, 044304 (2013)
  J. Sinclair, priv. comm. (2019)

E1, M1

- Inelastic electron scattering (e, e') :
  W.Mettner et al., Nucl. Phys. A473, 160 (1987)

M1, M2

- (p, p') at 160 MeV + ^{58}Ni(^{3}He,t)^{58}Cu:
  H.Fujita et al., Phys. Rev. C 75, 034310 (2007)

E1, IVSM1

IVSM1 Distribution
Shell model calculations and experiment

- Isospins from (p, p') + ^{58}Ni(^{3}He,t)^{58}Cu
  H.Fujita et al., Phys. Rev. C 75, 034310 (2007)
- Shell model calculations
  G. Martìnez-Pinedo
  R. Mancino
- GXPF1A and KB3G interaction
- Quenching factor 0.75
- 100 iterations

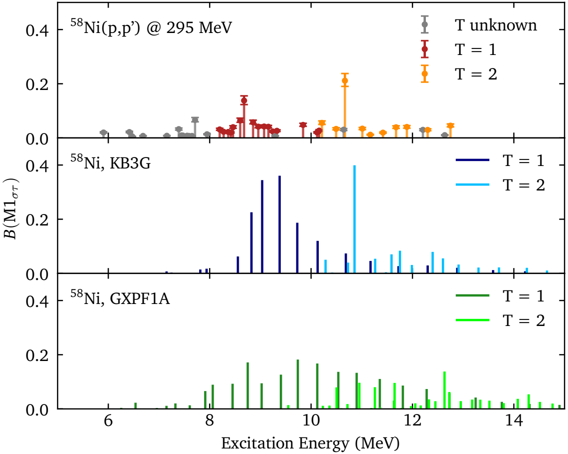

IVSM1 Running Sum
Shell model calculations and experiment

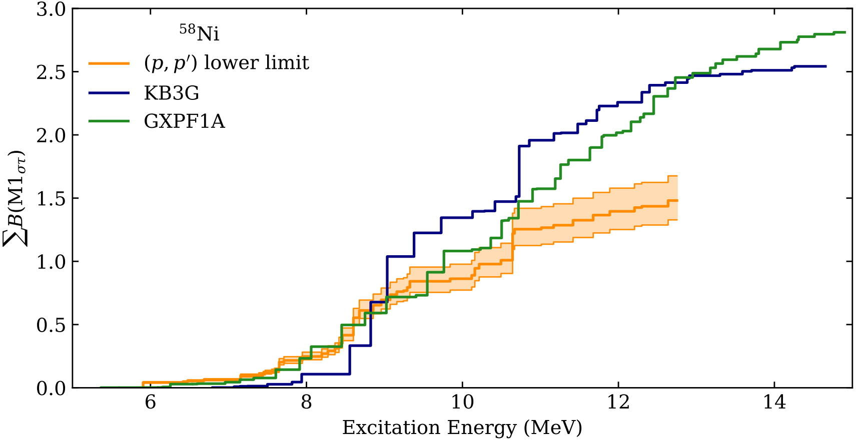

IVSM1 Running Sum
Shell model calculations and experiment

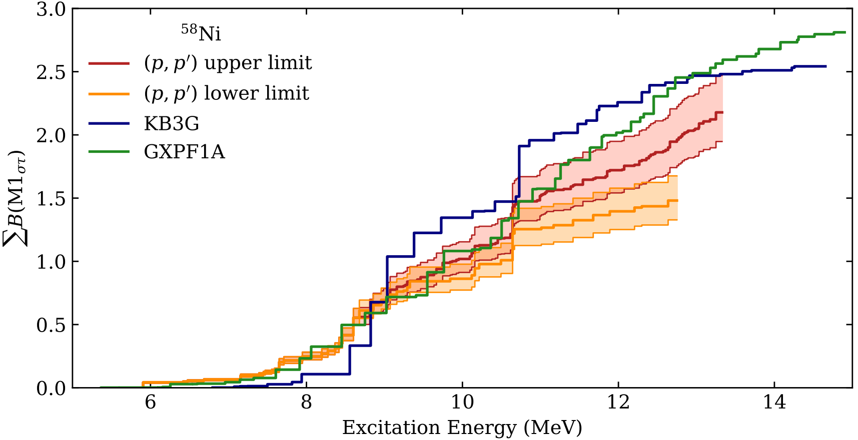

E1 and M1 strength

- (p, p'): conversion into electromagnetic $B(\mathrm{M1})$
  - Isoscalar contributions negligible
  - Pure spin excitation
  - J. Birkhan et al., Phys. Rev. C 93, 041302(R) (2016)
- (e, e') and (γ, γ'): Spin and orbital contributions

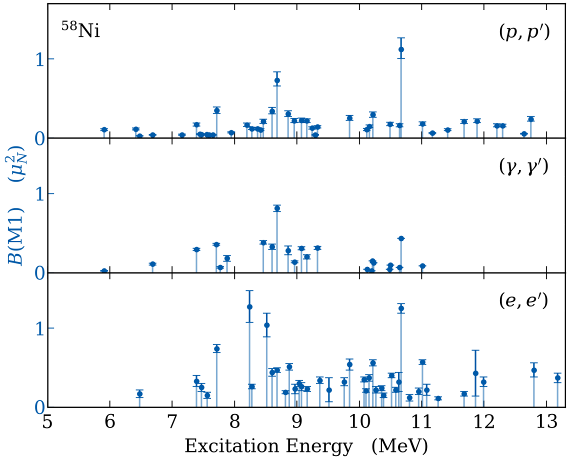

E1 and M1 strength

- (p,p'): conversion into electromagnetic $B(\mathrm{M1})$
  - Isoscalar contributions negligible
  - Pure spin excitation
  - J. Birkhan et al., Phys. Rev. C 93, 041302(R) (2016)
- (e,e') and (γ,γ'): Spin and orbital contributions
- $B(\mathrm{E1})$ in (p,p') enhanced compared to (γ,γ')

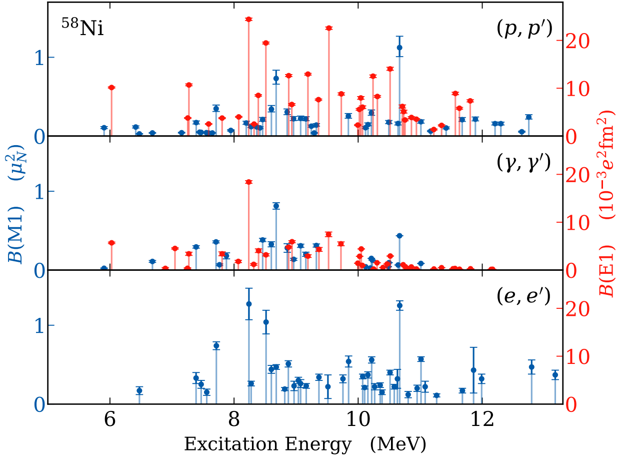

E1 and M1 strength

- $(\gamma, \gamma')/(p, p')$: E1 transitions
- (e, e') measured under backward angles
  - Sensitive to transverse cross section
  - M1, M2

? Electric transitions with a strong transverse component

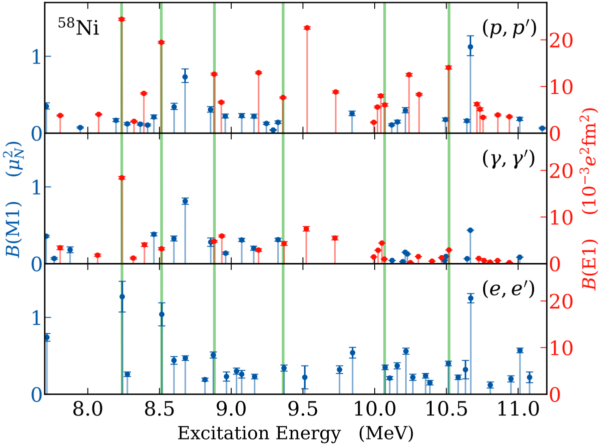

E1 and M1 strength

- ► $(\gamma, \gamma')/(p, p')$: E1 transitions
- ► (e, e') measured under backward angles
  - ▷ Sensitive to transverse cross section
  - ▷ M1, M2

? Electric transitions with a strong transverse component

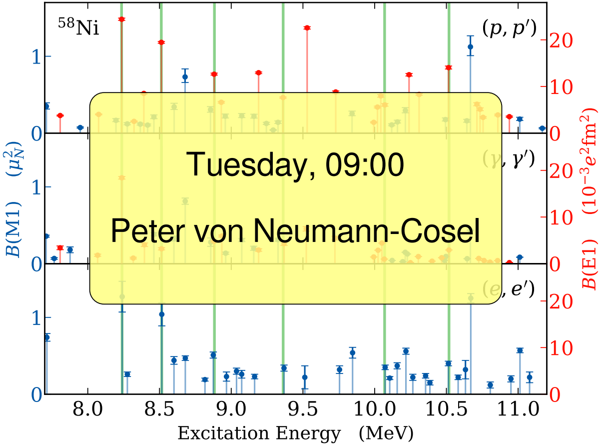

^{58}Ni Spectra

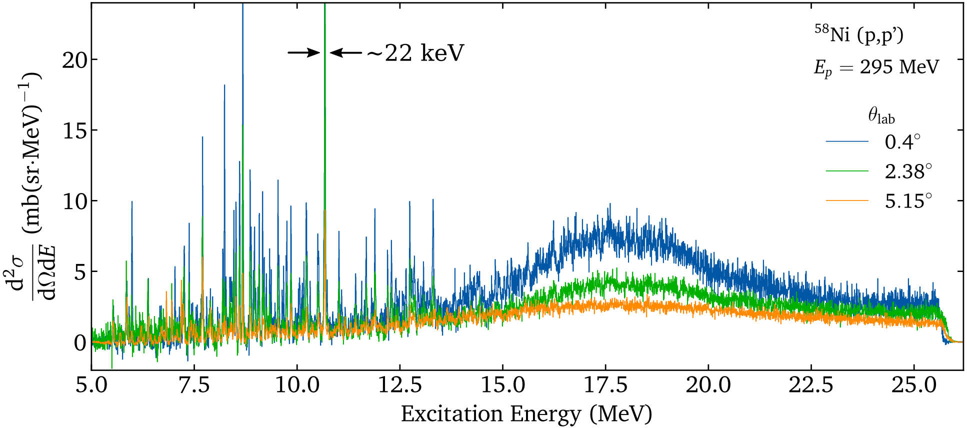

Multipole decomposition analysis

- Spectrum in 200 keV bins
- Fit of DWBA curves to experimental angular distributions

$$\frac{d\sigma}{d\Omega}(\theta_{cm}, E_x)\Big|_{Exp.} = \sum_{J^\pi} a^{J^\pi} \frac{d\sigma}{d\Omega}(\theta_{cm}, E_x, J^\pi)\Big|_{DWBA}$$

- χ^2_{red} weighted contribution for each multipolarity

$$\left\langle \frac{d\sigma}{d\Omega}(\theta, E_x)^{J^\pi} \right\rangle = \frac{\sum_i \omega_i \frac{d\sigma}{d\Omega}(\theta, E_x)_i^{J^\pi}}{\sum_i \omega_i} \quad \text{with} \quad \omega = \frac{1}{\chi^2_{red}}$$

- MDA uncertainty from weighted variance

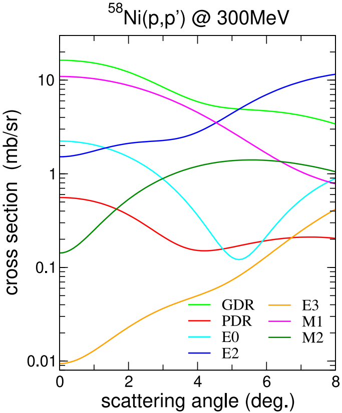

V. Yu. Ponomarev (2019)

Multipole decomposition analysis

- Subtraction of ISGMR and ISGQR
  Y.-W. Lui et al., Phys. Rev. C 73, 014314 (2006)
- Below 13 MeV: isovector spin-flip M1 resonance
- Phenomenological background from quasi-free scattering
  S. Bassauer et al., Phys. Rev. C 102, 034327 (2020)
- Above 20 MeV: large uncertainties
  - Limited input from theory

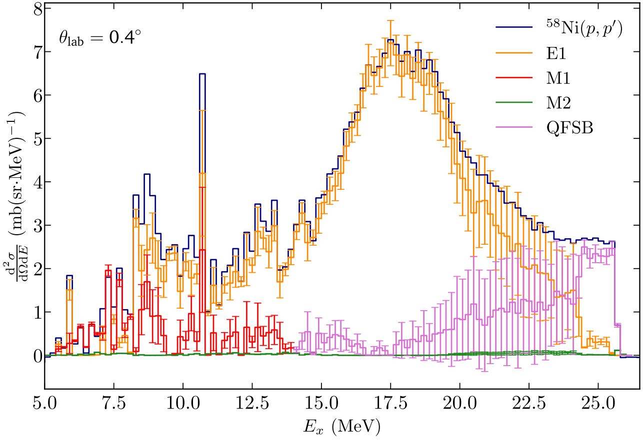

Results for ^{58}Ni

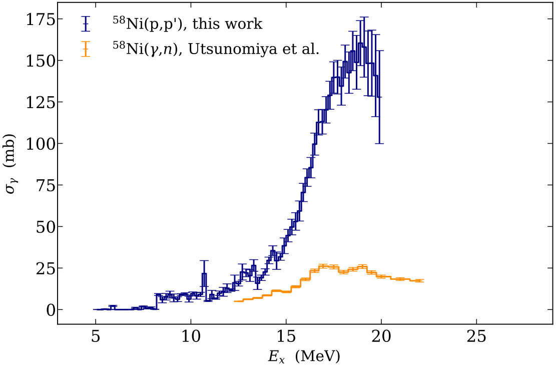

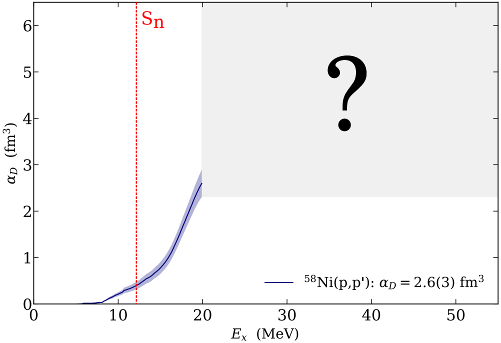

Systematics of the dipole polarizability

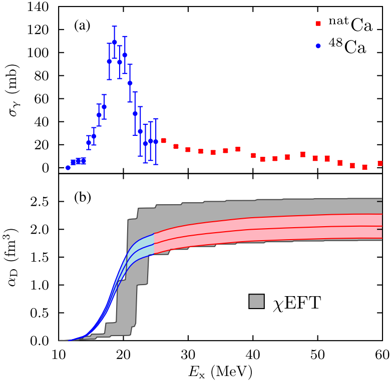

J. Birkhan et al.,
Phys. Rev. Lett. 118, 252501 (2017)

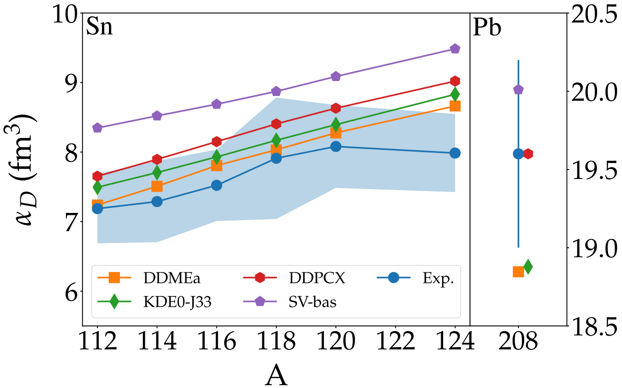

S. Bassauer et al., Phys. Lett. B 810, 135804 (2020)
A. Tamii et al. Phys. Rev. Lett 107, 062502 (2011)

Comparison to Migdal model

- Hydrodynamic model with interpenetraiting proton and neutron fluids

$$\alpha_D = \frac{e^2 R^2 A}{40 \cdot a_{\mathrm{sym}}} \propto A^{5/3}\,\mathrm{fm}^3$$

- a_{sym}: Symmetry energy parameter in the Bethe-Weizsäcker mass formula
- S.Dietrich and B.Bermann, At. Data Nucl. Data Tables 38, 199 (1988)

$$\alpha_D = 2.4 \times 10^{-3} \cdot A^{5/3}\,\mathrm{fm}^3$$

- Fit: $\alpha_D = 3.0(3) \times 10^{-3} \cdot A^{5/3}\,\mathrm{fm}^3$

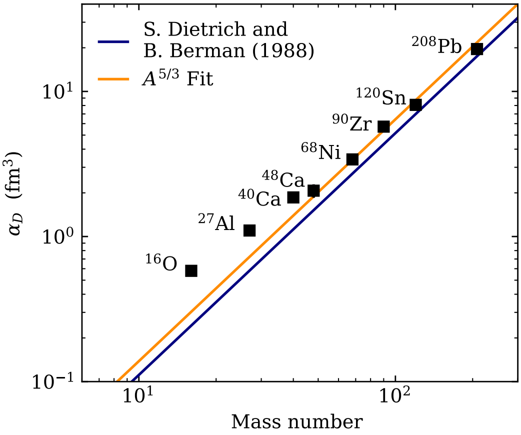

Comparison to Migdal model

- More realistic model: a_{sym} mass dependent

$$a_{\text{sym}}(A) = S_v\left(1 - \frac{\kappa}{A^{1/3}}\right), \quad \kappa = \frac{S_s}{S_v}$$

$$\alpha_D = \frac{0.0518 \cdot A^2}{S_v(A^{1/3} - \kappa)}\ \text{fm}$$

J.Tian et al., Phys. Rev. C 90, 024313 (2014) — $S_v = 28.3$ MeV, $\kappa = 1.27$

(I.) A.W. Steiner et al., Phys. Rep. 411, 325 (2005) — $S_v = 24.1$ MeV, $\kappa = 0.545$

(II.) A.W. Steiner et al., Phys. Rep. 411, 325 (2005) — $S_v = 27.3$ MeV, $\kappa = 1.68$

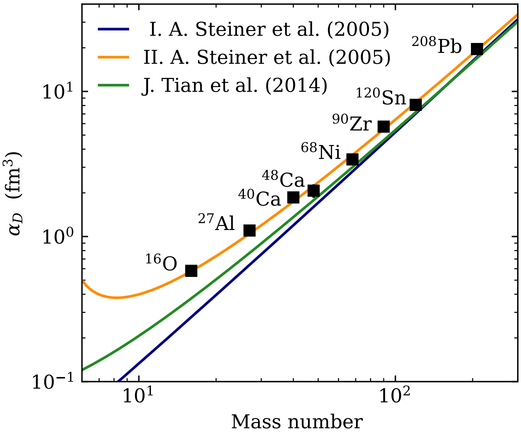

Comparison to Migdal model

- More realistic model: a_{sym} mass dependent

$$\alpha_D = \frac{0.0518 \cdot A^2}{S_v(A^{1/3} - \kappa)} \text{fm}^3, \quad \kappa = \frac{S_s}{S_v}$$

J.Tian et al., Phys. Rev. C 90, 024313 (2014)	$S_v = 28.3$ MeV, $\kappa = 1.27$
(I.) A.W. Steiner et al., Phys. Rep. 411, 325 (2005)	$S_v = 24.1$ MeV, $\kappa = 0.545$
(II.) A.W. Steiner et al., Phys. Rep. 411, 325 (2005)	$S_v = 27.3$ MeV, $\kappa = 1.68$
Fit	$S_v = 27.3(8)$ MeV, $\kappa = 1.69(6)$

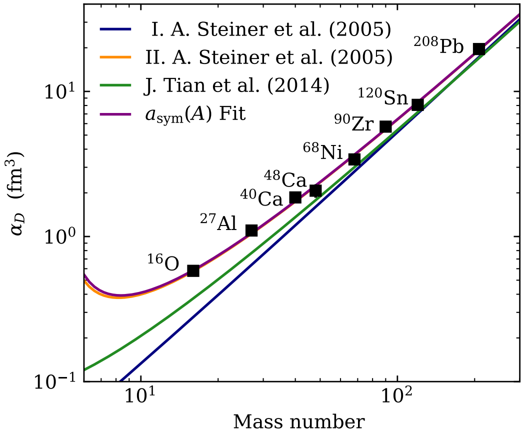

Summary

- Inelastic proton scattering at extreme forward angles is a tool to probe the dipole response in nuclei

- Electric and magnetic dipole response of ^{58}Ni

- Experimental systematic of the dipole polarizability:
  ^{40,48}Ca, ^{68}Ni, ^{90}Zr, ^{112,114,116,118,120,124}Sn, ^{208}Pb,
  and in the near future ^{58}Ni

Outlook

- Constraints for the symmetry energy parameters and neutron skin thickness
- Test of ab-initio calculations of E1 response and dipole polarizability

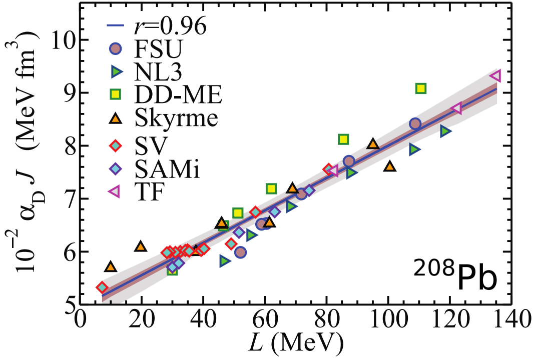

Outlook

- Constraints for the symmetry energy parameters and neutron skin thickness
- Test of ab-initio calculations of E1 response and dipole polarizability

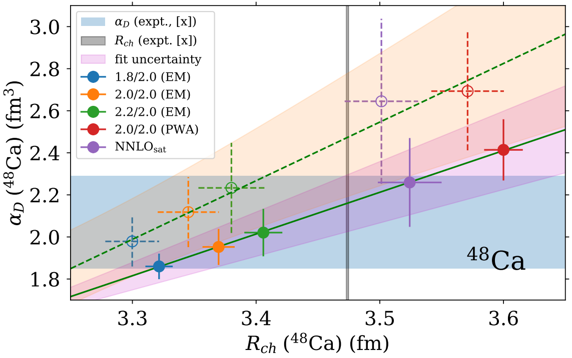

Thank you for your attention!

Multipole decomposition analysis